Taguchi Approach of Dissimilar Welds for AISI 4340 Steel and 304 Austenitic Stainless Steel

Amir Arifin[*]*, Gunawan, Andika Akbar Pratama*
Department of Mechanical Engineering, Faculty of Engineering,
Sriwijaya University, Indralaya, 30662, Sumatera Selatan, Indonesia
**amir@unsri.ac.id*

Alim Mardhi
Research Center for Nuclear Reactor Technology,
National Research and Innovation Agency (BRIN), Kompleks PUSPIPTEK,
Gedung 80, Serpong, Tangerang Selatan 15314 Banten, Indonesia

ABSTRACT

Dissimilar metals welding using shielded metal arc welding (SMAW) has been widely used in various industries such as automotive, maritime, transportation, and offshore structures. In this work, the Taguchi approach was applied for improving the tensile strength of dissimilar welding between AISI 4340 steel and 304 Austenitic stainless steel. The effects of four welding factors: electrode type, welding current, joint type, and welding speed on the tensile strength were studied. The various factors were assigned to an L9 orthogonal array, and analysis of variance (ANOVA) was utilized to determine a significant contributing factor. It was found that electrode type and current welding factors significantly affect tensile strength. The optimum condition parameters for tensile strength were achieved with an electrode type (E309), welding current (110 A), joint type (II), and welding speed (2 cm/min).

Keywords: *Stainless Steel 304; Dissimilar Welding; AISI 4340; ANOVA*

Introduction

The dissimilar joint of carbon steel to stainless steel has a widespread application in numerous sectors, such as nuclear power plants, automotive, oil and gas, petrochemical, and petroleum. Steel with various grades is one of the most widely used materials in various industries, which is very much needed

ISSN 1823-5514, eISSN 2550-164X
Received for review: 2022-04-10
Accepted for publication: 2022-07-22
Published: 2022-09-15

for heavy construction in the industry. Integrating multiple types of steel in heavy construction in an industry is unavoidable. Stainless steel can be used to achieve the non-corrosive behaviour of a structure. However, using stainless steel in all fields is not cost-effective for the industry. Hence low alloy steels can be used in conditions where corrosion is not a significant consideration to achieve an optimal design. Dissimilar welding in the industry plays an essential role in improving performance capability, high-efficiency formability, and minimizing lost costs [1]-[4].

In welding dissimilar metals, the properties of three metals must be recognized: the two metals being joined, and the filler metal used to join them. Each metal has unique mechanical and physical qualities that necessitate different welding requirements. There may be occasions when optimal control for one metal is not desired for another. In this circumstance, a compromise is essential. This is one reason why the development of dissimilar metal welding processes generally necessitates more research than conventional comparable metal welding procedures.

Dissimilar metal welding is an innovative method of joining two dissimilar metals with differing chemical compositions, melting temperatures, and thermal expansion coefficients [5]-[8]. Joining two dissimilar metals can be performed in various methods. Each welding method will have advantages and disadvantages over other processes. Dissimilar welded joints should have sufficient strength and ductility to prevent failure of the welded joint.

The microstructural and mechanical properties of joints are significantly influenced by welding parameters such as the voltage, welding current, arc travel rate, number of passes, root gap, and polarity of the electrode, etc [9]- [10]. Furthermore, the filler material and electrode type used in the SMAW method will affect the weld quality [11]. The selection of an adequate filler wire is the most challenging aspect of dissimilar metal welding. Unsuitable filler wire selection can produce metallurgical issues such as liquidation cracking at heat affected zone, weld solidification cracking, and occurring undesired secondary phases [12].

Many researchers are studying the joining of different materials and trying to figure out the best welding methods, optimum welding conditions, and optimum mechanical properties of the dissimilar joint [9][13][14]. Some welding methods, such as gas metal arc welding (GMAW), gas tungsten arc welding (GTAW), submerged arc welding (SAW), fusion welding, pressure welding, diffusion welding, brazing, and soldering have been utilized to join dissimilar materials [11]. Shielded metal arc welding (SMAW) is a versatile welding method commonly recognized in the fabrication of various metals since it considerably increases the weldments' quality.

AISI 4340 and stainless steel 304 have received much attention since they provide higher corrosion resistance and mechanical characteristics. AISI 4340 steel is low-alloy steel with a medium carbon content recognized for its toughness and strength in large sections. AISI 4340 steel is categorized as

nickel-chromium-molybdenum steel [15]. The AISI 4340 steel has impact resistance as well as wear and abrasion resistance in hardened conditions. AISI 4340 steel properties offer good ductility in the annealed condition, allowing it to be bent or formed. The 304 austenitic stainless steel is the most versatile and widely utilized. The former term 18/8 refers to the nominal composition of type 304, which is 18% chromium and 8% nickel. It has been applied widely in chemical manufacturing, pressure vessels, medical equipment, commercial kitchens, and food production. 304 austenitic stainless steel has excellent environmental corrosion resistance and different corrosive media. However, it is prone to corrosion caused by chloride solutions or saline environments like the sea. Pitting is corrosion triggered by chloride ions that can spread beneath protective chromium barriers and degrade internal structure.

In conventional experimental methods analyses, industrial process variables were optimized by varying one variable while maintaining the other constantly. This procedure is expensive, time-consuming, and does not produce satisfactory results. the Taguchi method is a robust methodology that has been shown to improve the performance of manufacturing processes [16]-[18]. Taguchi developed an orthogonal array matrix to design the experiments. This method uses an orthogonal array dependent on the number of levels and factors involved in the process.

This research work investigates the contribution effects and optimization conditions of welding parameters, i.e., welding parameters, namely electrode type, welding current, joint type, and welding speed. The Taguchi method with L9 orthogonal array (OA) was applied to design the controllable parameters experiment and response variables. The optimal condition for maximizing tensile strength was pursued with the signal-to-noise (S/N) ratio value from the Taguchi method. Analysis of variance (ANOVA) statistically examined the significance level of each controllable parameter. Finally, the comparison process of the results from the experiment and measured values was prepared for confirmation and validation in this research work.

Methodology

The Taguchi method was chosen to determine the influence of the process parameters and the interaction between the process parameters and multi-output response. The Taguchi method provides an efficient, structured, and reliable method for design, performance, quality, and cost optimization [17][19][20]. The significance of the process parameters on the output response was determined using ANOVA. In this work, parameter processes were designed to refer to an orthogonal array of L9, which consists of four welding parameters comprising electrode type (E308, E309, and E312), welding current (90, 100, and 110 A), joint type (V, II, and IV), and welding

speed (4, 2 and 1 cm/min) (Table 1). The experimental layout of nine experimental runs over three levels and four factors can be presented in Table 2.

Table 1: Factors and levels for the welding process

Parameters	Level 1	Level 2	Level 3
Electrode type (A)	E308	E309	E312
Welding current (B)	90	100	110
Joint type (C)	V	II	VI
Welding speed (D)	4	2	1

304 austenitic stainless steel and AISI 4340 steel were chosen as the two steel grades for this study. The sample plates were machined into 162 × 110 ×10 mm dimensions. The joining process was conducted utilizing the SMAW method with various electrode types. Furthermore, universal testing machine type RAT-30P was used to analyze tensile strength.

Table 2: Experimental layout and factors distribution of the orthogonal array

Exp. No.	Factor				Experimental Value			
	A	B	C	D	Electrode type	Welding current (A)	Joint type	Welding speed (cm/min)
1	1	1	1	1	E 308	90	V	4
2	1	2	2	2	E 308	100	II	2
3	1	3	3	3	E 308	110	VI	1
4	2	1	2	3	E 309	90	II	1
5	2	2	3	1	E 309	100	VI	4
6	2	3	1	2	E 309	110	V	2
7	3	1	3	2	E 312	90	VI	2
8	3	2	1	3	E 312	100	V	1
9	3	3	2	1	E 312	110	II	4

The raw materials were properly cleaned to remove contamination such as rust, dust, oil, and moisture in order to avoid welding problems caused by contamination. For the tensile test, the specimens were machined from the weld plates refer to JIS Z 2201 standard. Figure 1 shows the schematic of the tensile specimen geometry.

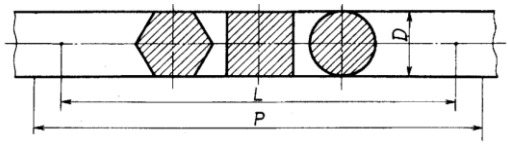

Figure 1: The tensile specimen used in the present study according to JIS Z 2201 standards

where;

D = Diameter or width across flats

L = Gauge length

P = Distance between grips

size of specimen:

L = 8.D

P = L + 2D Approx.

For hardness and metallography analysis, weld joint specimens were polished using the silicon carbide sandpaper sheets with various grit sizes from 120 to 1200, then by final mechanical polishing with polishing paste. To display the microstructures at the specified zones of weldments, a mixture of 2% Nital in alcohol at room temperature and 50% HCL in H2O for carbon steel and SS304, respectively. Optical investigations were carried out using STM6-LM measuring microscope Olympus. Hardness measurements have been carried out along the base metal area, heat affected zone, and fusion zone using type VKH-2E Vickers hardness test based on JIS B7725 as standard. To analyze changes in the welding joint microstructure after welding. Furthermore, X-Ray Diffraction (XRD) observations were performed using Rigaku MiniFlex 600 to determine the phases generated in fusion zone.

Results and Discussion

The tensile strength of the weld joint was measured through the tensile test referring to orthogonal array L9 with three replications. The tensile test results can be seen in Table 3. The output of the experimental value is used to obtain the combination of optimal parameters. Here the objective is to improve the tensile strength of dissimilar weld joints. Taguchi method with "the larger the better" is utilized to obtain an optimum condition of the welding process. From the response graphs illustrated in Figure 2 the highest yield of the tensile strength could be achieved at the combined settings of A2, B3, C2, and D2, i.e., electrode type of E309, welding current of 110 A, joint type of II, and welding speed of 2 cm/min. This combination of settings was not examined in the experiment, indicating that the orthogonal experiment may have

successfully identified the optimum factors in the multi-dimensional factor space.

The relative significance of the factors was determined using the ANOVA approach. ANOVA is a data table showing the relative influences of factors and interactions in the columns of an orthogonal array.

Table 3: Tensile strength of weld joint

Ext.	Factors				Replication, tensile Strength (MPa)			Average
	A	B	C	D				
1	1	1	1	1	338,313	165,761	251,987	252,020
2	1	2	2	2	186,481	193,172	174,614	184,756
3	1	3	3	3	168,603	148,868	227,632	181,701
4	2	1	2	3	293,858	485,364	353,864	377,695
5	2	2	3	1	257,263	280,464	196,384	244,704
6	2	3	1	2	446,192	543,439	461,360	483,664
7	3	1	3	2	293,416	261,656	288,291	281,121
8	3	2	1	3	836,877	214,764	362,812	471,484
9	3	3	2	1	430,873	512,871	395,818	446,521

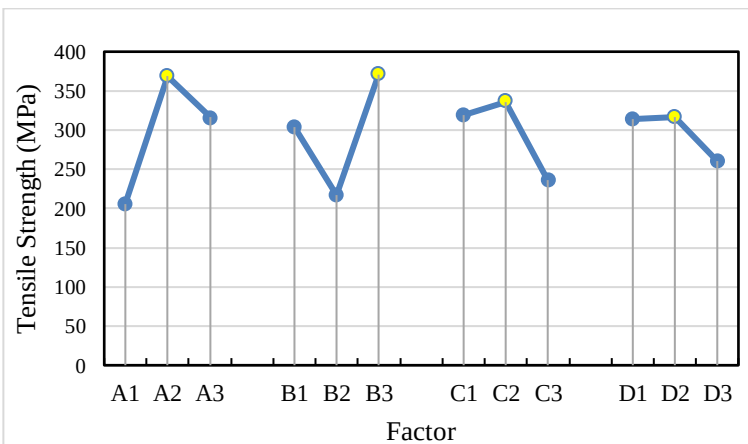

Figure 2: Response graph of tensile strength against various factors

The F-table utilized is the estimated point of the F distribution with the probability value (F0.05), where (F0.05; N1 = 2; N2 = 18) = 3.55. The ANOVA result shows that factor (D) is not significant enough to contribute to tensile strength because its F ratio is less than the F table. Furthermore, the

"pooling" procedure was carried out to minimize overestimation, as shown in Table 4.

Table 4: ANOVA

Source	Pooling	SS	DF	F-ratio	% Ratio	F-table
A		123776.86	2	8.30	28%	3.55
B		107322.35	2	7.20	23%	3.55
	Y	-	-	-	-	-
	Y	-	-	-	-	-
	Y	-	-	-	-	-
Pooled		163997.53	22	1	49%	
SSt		395096.74	26		100%	
Mean		2380934.83	1			
SS_{tot}		2776031.56	27			

Pooling procedure revealed that factors A and B significantly improve the strength of the welded joint as shown by the much higher F ratio. The E309 electrode has a high Cr concentration and a modest quantity of ferrite, which results in superior fracture resistance. The amount of composition and type of alloys such as chromium, manganese, and molybdenum contained in each electrode used has a significant influence on the mechanical properties of the welded joint, as shown in Figure 2.

After establishing the optimum factor level, the confidence interval value for the mean under optimal conditions must be determined. The estimated optimum condition for the mean value for all data is y = 296.9558407, and then the calculation is as follows:

$$\mu_{estimated} = \bar{y} + (\overline{A2} - \bar{y}) + (\overline{B3} - \bar{y})$$

$$\mu_{estimated} = 442.3601593$$

$$CI_{mean} = \pm \sqrt{F_{\alpha;v1;v2} \times MS_e \times \left|\frac{1}{neff}\right|}$$

where:

$$neff = \frac{total\ number\ of\ experiment}{sum\ of\ degrees\ of\ freedom\ used\ in\ estimate\ of\ mean}$$

$$CI_{mean} = \pm \sqrt{F_{\alpha;v1;v2} \times MS_e \times \left|\frac{1}{neff}\right|}$$

$$CI_{mean} = \pm 77.04503511$$

The following is the result of the confidence interval obtained:

$$\mu_{estimated} - Cl_{mean} \leq \mu_{estimated} \leq \mu_{estimated} + Cl_{mean}$$

$$365.315 \leq \mu_{estimated} \leq 519.405$$

The tensile strength value using optimum parameter; electrode type of E309, welding current of 110 A, II joint type, and welding speed of 2 cm/min was estimated in the range 365. 315 MPa and 519.405 MPa. In the fusion zone, there is an interaction between the composition of three types of materials: AISI 4340 steel, 304 austenitic stainless steel and filler. The heat flow strongly influences the phase transformation in the fusion zone and heat affected zone during welding. One of the parameters that affect the heat flow is the welding current. Generally, austenitic stainless steels with 5-10% δ-ferrite are significantly more resistant to solidification cracking than fully austenitic stainless steels [21]. Furthermore, when exposed to high temperatures (600-850 °C), δ-ferrite can change to brittle σ-ferrite, affecting the mechanical properties of austenitic stainless steels unless the ferrite percentage is kept low. Referring to ANOVA, the parameters that contribute to tensile strength are the type of electrode and welding current. These two parameters play an important role in determining the formation of the phase, which determines the tensile strength produced.

The weld hardness joint profile distribution using the E309 type through the Vickers method can be seen in Figure 2. Hardness value was examined on the heat-affected zone, fusion zone, and unaffected base metal zone of SS 304 and AISI 4340.

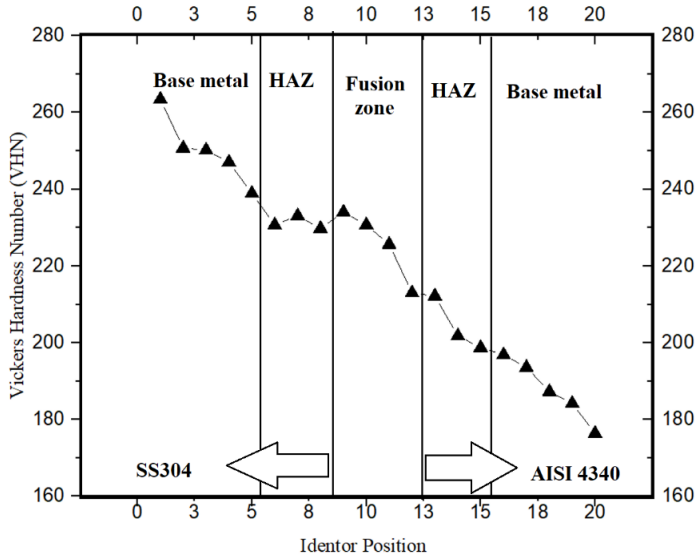

Figure 3: Hardness test profile on optimum parameter sample

Figure 3 shows the hardness profile of the weld joint of SS 304 and AISI 4340. Maximum hardness value was obtained on SS 304 zone (250.5 VHN) and minimum hardness value on AISI 4340 (187.7 VHN). The combination SS 304, AISI 43040, and E309 electrode composition on fusion zone were obtained hardness value on 225.9 VHN on the heat affected zone of AISI 4340, and there was an increase in hardness value compared to areas that were not exposed to heat. The increasing hardness value in this zone occurs due to grain refinement caused by the fast-cooling rate of heat input. However, the hardness value decreases on the SS 304 side due to the thermal cycle effect during welding.

Brittle intermetallic phases are commonly seen in dissimilar welding, particularly involving stainless steel. In addition, steel phases have been discovered that can improve the weld joint strength or vice versa. These phases can occur due to thermal cycling, material composition, and filler utilized during welding. In terms of phase formation at the fusion zone, the Schaeffler diagram is widely used to predict phase formation in the fusion zone after welding [22][23]. The Schaeffler diagram is an essential tool for estimating the composition of austenitic Cr-Ni steel welds with carbon concentrations as low as 0.12%. All concentrations of composition are represented as a percentage of the total weight. Figure 4 shows the formation of phases prediction due to the interaction of the alloy composition used, which refers to the calculation of Ni_{eq} and Cr_{eq}.

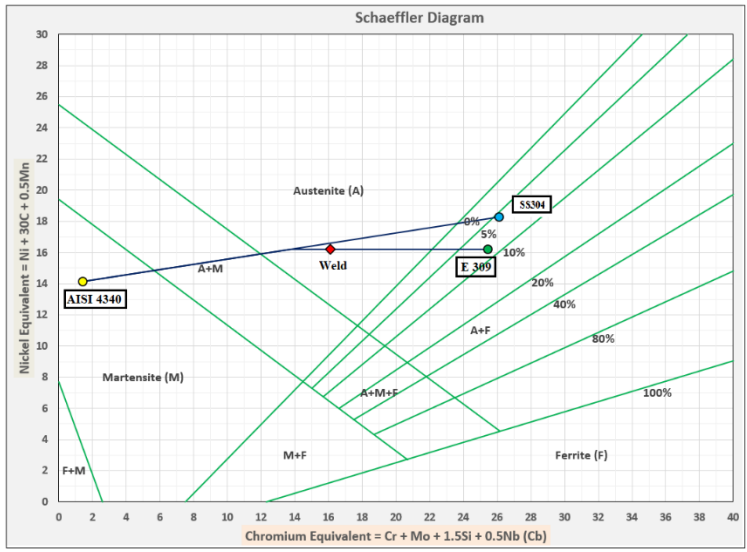

Figure 4: AISI 4340 steel and 304 austenitic stainless steel fusion zone prediction with E309 electrode

Figure 4 shows phases prediction optimum parameter AISI 4340 steel and 304 austenitic stainless steel weld joint using E309. In this work, due to the square groove weld (weld joint type II) being an optimum parameter, the approximate dilution ratios are 20% and 80% for filler and base metal, respectively [21]. The Schaeffler diagram reveals that the utilization of the E309 electrode for welding AISI 4340 steel and 304 austenitic stainless steel exhibits austenite microstructure, as shown in Figure 4. The fusion zone with austenite microstructure in this condition tends to be prone to hot cracking. Low-melting eutectics, such as S and P, and alloy elements like Ti and Nb, produce hot cracking in stainless steel welds [24]. Ferrite number (FN) are based on magnetic measurement, which are possible because the body center cubic delta ferrite is ferromagnetic, while the face center cubic austenite is not. In this work, FN prediction was not valid to carried out due to the calculation of weld metal composition (Cr_{eq} = 16.1 and Ni_{eq} = 16.2) falls outside the isoferrite line of DeLong diagram [25]. Position of weld metal composition can be seen on the Figure 5.

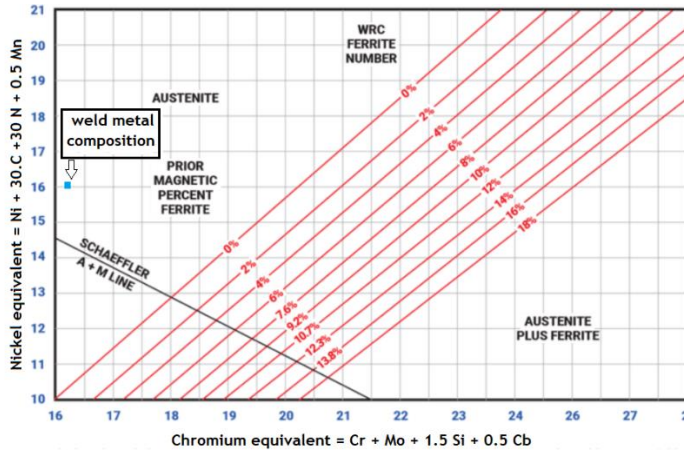

Figure 5: DeLong diagram for calculating ferrite number

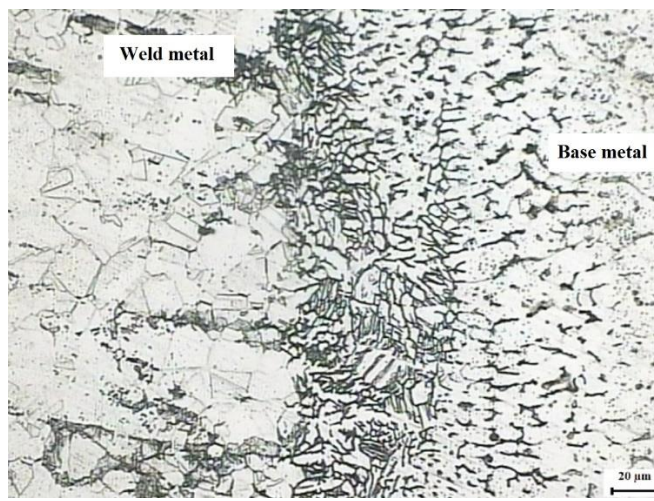

Figure 6: Epitaxial growth near the fusion boundary of SS 304 welded with AISI 4340 filler E309

At the fusion line, three grains are visible in the base metal; all dendrites develop from each grain point in one direction, which differs from grain to grain. Epitaxial development near the fusion line may be seen in the welds in Figure 6. Epitaxial growth can also occur when the workpiece is composed of many phases, as shown in Figure 6. At the fusion line from the base metal to the weld metal, both austenite and ferrite grow epitaxially. The presence of

heat input during the welding process contributed significantly to grain size and phase formation in the fusion zone and HAZ. Some Widmanstätten ferrite structures was observed at HAZ. It is separated into two zones: the normalized zone, which has been heated to slightly over A3, and the overheated zone, which has been heated to much above A3 and up to the melting point of the material. The grain enlargement in the overheated zone is substantial, and the structure is partially Widmanstätten-oriented.

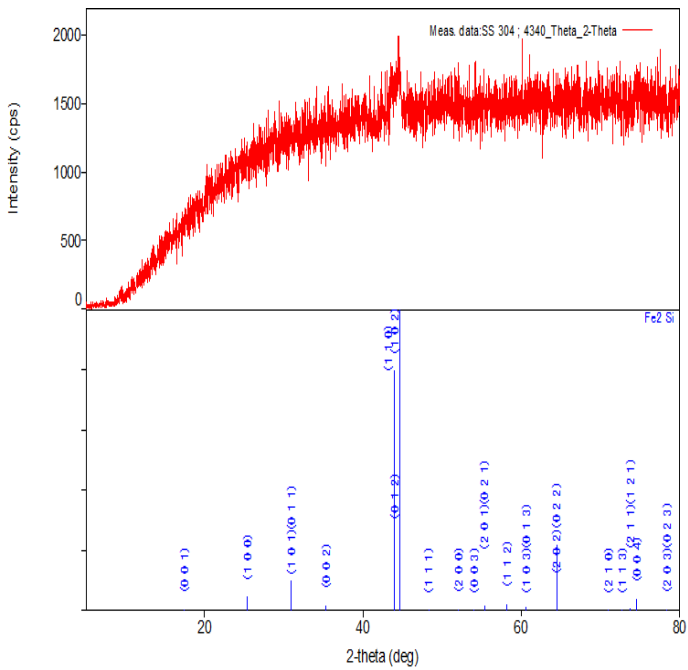

Figure 7: XRD analysis of AISI 4340 and SS 304 weld joint

Figure 7 shows the phase results in the fusion zone of AISI 4340 and SS 304. XRD results were investigated refer to Crystallography Open Database (COD). It can be seen that the red lines show the crystallization contained in the joint. The higher the intensity, the higher the crystallization. On the other hand, the lower the peak list, the lower the crystallization. The graph above shows the highest peak list, namely Fe_2Si. The data shows the highest peak in the weld metal area, 44.45. In XRD observations, by detecting an angle of 2θ, the phase content is formed. It can be seen that at the highest intensity, 44.45 contains a gamma phase (γ -Fe). Several peak lists show the austenite phase at intensity 30.00, 44.45, and 75.00. The α -ferrite (α-Fe) phase is shown on the peak list with an intensity of 45.00 and 65.00.

Conclusion

Using the Taguchi method, process parameter optimization improves the tensile strength of dissimilar welding of AISI 4340 and SS 304. The optimum condition parameters for tensile strength were obtained with an electrode type (E309), welding current (110 A), joint type (II), and welding speed (2 cm/min). ANOVA showed that electrode type and welding current play an essential role in improving tensile strength. The Schaeffler diagram reveals that the utilization of optimum welding parameters for AISI 4340 steel and 304 austenitic stainless steel exhibits austenite microstructure.

Acknowledgment

The authors would like to convey their great appreciation to Sriwijaya University for supporting this research.

References

[1] F. Dokme, M. Kulekci, and U. Esme, "Microstructural and Mechanical Characterization of Dissimilar Metal Welding of Inconel 625 and AISI 316L," *Metals,* vol. 8, no. 10, pp. 1-18, 2018.

[2] H. Wang, G. Qin, P. Geng, and X. Ma, "Interfacial microstructures and mechanical properties of friction welded Al/steel dissimilar joints," *Journal of Manufacturing Processes,* vol. 49, pp. 18-25, 2020.

[3] Y. Zhang, R. Li, P. Chen, X. Li, and Z. Liu, "Microstructural evolution of Al2Cu phase and mechanical properties of the large-scale Al alloy components under different consecutive manufacturing processes," *Journal of Alloys and Compounds,* vol. 808, pp. 1-9, 2019.

[4] V. Patel, W. Li, G. Wang, F. Wang, A. Vairis, and P. Niu, "Friction Stir Welding of Dissimilar Aluminum Alloy Combinations: State-of-the-Art," *Metals,* vol. 9, no. 3, pp. 1-19, 2019.

[5] Afriansyah and A. Arifin, "Dissimilar metal welding using Shielded metal arc welding: A Review," *Technology Reports of Kansai University,* vol. 62, no. 04, 2020.

[6] K. Devendranath Ramkumar *et al.*, "Metallurgical and mechanical characterization of dissimilar welds of austenitic stainless steel and super-duplex stainless steel – A comparative study," *Journal of Manufacturing Processes,* vol. 19, pp. 212-232, 2015.

[7] H. Purwanto, M. Dzulfikar, I. Syafaat, S. Imanu, and N. Kholis, "Effects of Pressure in Continuous Drive Friction Welding on Aisi 304 and A36," *MM Science Journal,* vol. 2020, no. 4, pp. 4138-4142, 2020.

[8] Y. Fang, X. Jiang, D. Mo, D. Zhu, and Z. Luo, "A review on dissimilar metals' welding methods and mechanisms with interlayer," *The International Journal of Advanced Manufacturing Technology,* vol. 102, no. 9-12, pp. 2845-2863, 2019.
[9] B. K. Khamari, S. S. Dash, S. K. Karak, and B. B. Biswal, "Effect of welding parameters on mechanical and microstructural properties of GMAW and SMAW mild steel joints," *Ironmaking & Steelmaking,* vol. 47, no. 8, pp. 844-851, 2019.
[10] M. Vahman, M. Shamanian, M. A. Golozar, A. Jalali, M. A. Sarmadi, and J. Kangazian, "The Effect of Welding Heat Input on the Structure–Property Relationship of a New Grade Super Duplex Stainless Steel," *steel research international,* vol. 91, no. 1, pp. 1900347-1900347, 2020.
[11] M. Khan, M. W. Dewan, and M. Z. Sarkar, "Effects of welding technique, filler metal and post-weld heat treatment on stainless steel and mild steel dissimilar welding joint," *Journal of Manufacturing Processes,* vol. 64, pp. 1307-1321, 2021.
[12] M. F. Buchely, H. A. Colorado, and H. E. Jaramillo, "Effect of SMAW manufacturing process in high-cycle fatigue of AISI 304 base metal using AISI 308L filler metal," *Journal of Manufacturing Processes,* vol. 20, pp. 181-189, 2015.
[13] D. Kumar Singh, G. Sahoo, R. Basu, V. Sharma, and M. A. Mohtadi-Bonab, "Investigation on the microstructure—mechanical property correlation in dissimilar steel welds of stainless steel SS 304 and medium carbon steel EN 8," *Journal of Manufacturing Processes,* vol. 36, pp. 281-292, 2018.
[14] I. A. Daniyan, K. Mpofu, and A. O. Adeodu, "Optimization of welding parameters using Taguchi and response surface methodology for rail car bracket assembly," *The International Journal of Advanced Manufacturing Technology,* vol. 100, no. 9-12, pp. 2221-2228, 2018.
[15] Gunawan and A. Arifin, "Intergranular Corrosion and Ductile-Brittle Transition Behaviour in Martensitic Stainless Steel," *Indonesian Journal of Engineering and Science,* vol. 2, no. 3, pp. 031-041, 2021.
[16] A. Arifin *et al*., "Optimization of Angular Distortion on Weld Joints Using Taguchi Approach," *Jurnal Kejuruteraan,* vol. 31, no. 1, pp. 19-23, 2019.
[17] N. Ghosh, P. K. Pal, and G. Nandi, "GMAW dissimilar welding of AISI 409 ferritic stainless steel to AISI 316L austenitic stainless steel by using AISI 308 filler wire," *Engineering Science and Technology, an International Journal,* vol. 20, no. 4, pp. 1334-1341, 2017.
[18] N. Y. Mahmood and A. H. Alwan, "Mechanical properties improvement of MIG welding steel sheets using Taguchi method," *Australian Journal of Mechanical Engineering,* pp. 1-8, 2019.
[19] K. Hafeez, H. Rowlands, G. Kanji, and S. Iqbal, "Design optimization using ANOVA," *Journal of Applied Statistics,* vol. 29, no. 6, pp. 895-906, 2002.

[20] R. Unal and E. B. Dean, "Taguchi approach to design optimization for quality and cost: an overview.," presented at the 13th Annual Conference of the International Society of Parametric Analysts, ISPA, New Orleans, LA., 1991.
[21] S. Kou, *Welding Metallurgy*. John Wiley & Sons, Inc, 2003.
[22] M. Pouranvari and S. P. H. Marashi, "Dissimilar Spot Welds of AISI 304/AISI 1008: Metallurgical and Mechanical Characterization," *steel research international*, vol. 82, no. 12, pp. 1355-1361, 2011.
[23] S. D. Brandi and C. G. Schön, "A Thermodynamic Study of a Constitutional Diagram for Duplex Stainless Steels," *Journal of Phase Equilibria and Diffusion*, vol. 38, no. 3, pp. 268-275, 2017.
[24] V. Shankar, T. P. S. Gill, S. L. Mannan, and S. Sundaresan, "Solidification cracking in austenitic stainless steel welds," *Sadhana*, vol. 28, 2003.
[25] J. C. Lippold and D. J. Kotecki, *Welding Metallurgy and Weldability of Stainless Steels*. John Wiley & Son, 2005.